

Seasonal Encoder-Decoder Architecture for Forecasting

Avinash Achar^{*§}, Soumen Pachal[§].

Abstract—Deep learning (DL) in general and Recurrent neural networks (RNNs) in particular have seen high success levels in sequence based applications. This paper pertains to RNNs for time series modelling and forecasting. We propose a novel RNN architecture capturing (stochastic) seasonal correlations intelligently while capable of accurate multi-step forecasting. It is motivated from the well-known encoder-decoder (ED) architecture and multiplicative seasonal auto-regressive model. It incorporates multi-step (multi-target) learning even in the presence (or absence) of exogenous inputs. It can be employed on single or multiple sequence data. For the multiple sequence case, we also propose a novel greedy recursive procedure to build (one or more) predictive models across sequences when per-sequence data is less. We demonstrate via extensive experiments the utility of our proposed architecture both in single sequence and multiple sequence scenarios.

Index Terms—Recurrent Neural Networks; Encoder-Decoder; Seq2Seq; time-series; Seasonal modelling;

I. Introduction

Deep recurrent neural networks have seen tremendous success in the last decade across domains like NLP, speech and audio processing [1], computer vision [2], time series classification, forecasting and so on. In particular, it has achieved state-of-art performance (and beyond) in tasks like handwriting recognition [3], speech recognition [4], [5], machine translation [6], [7] and image captioning [8], [9], to name a few. A salient feature in all these applications that RNNs exploits during learning is the sequential aspect of the data.

In this paper, our focus is on classical time-series, specifically the forecasting issue. The earliest attempts on employing RNNs for time series forecasting happened more than two decades ago [10], where RNNs were viewed as candidate nonlinear ARMA models. The main advantage of RNNs vs a feed-forward structure in building non-linear AR models is the weight sharing across time-steps, which keeps the number of weight parameters independent of the order of auto-regression. The early plain RNN unit was further enhanced with LSTM units [11], [12] which increased their ability for long-range dependencies and mitigated the vanishing gradient problem to an extent. With the exploding, ever-increasing data (sequential) available across domains like energy, transportation, retail, finance etc., accurate time-series forecasting continues to be an active research area. In particular, RNNs continue to be one of

the widely preferred predictive modelling tools for time-series forecasting [13].

Encoder-Decoder (ED) OR Seq2Seq architectures used to map variable length sequences to another variable length sequence were first successfully applied for machine translation [6], [7] tasks. From then on, the ED framework has been successfully applied in many other tasks like speech recognition [14], image captioning etc. Given the variable length Seq2Seq mapping ability, ED framework can be naturally utilized for multi-step (target) learning and prediction where target vector length can be independent of input vector length.

A. Contributions

Seasonal ARMAX models [15] are generalizations of ARMAX models which additionally capture stochastic seasonal correlations in the presence of exogenous inputs. While there are many non-linear variants of linear ARX or ARMAX models, there is no explicit non-linear variant of the SARMAX linear statistical model, which is capable of accurate multi-step (target) learning & prediction to the best of our knowledge. Existing related DL works either (1) consider some form of the ED approach for multi-step time-series prediction with exogenous inputs, without incorporating stochastic seasonal correlations [16], (2) many-to-many RNN architecture with poor multi-step predictive ability [17], [18], (3) incorporate stochastic seasonal correlations using additional skip connections via a non-ED predictive approach [19] to emphasize correlations from one cycle (period) behind, (4) capture deterministic seasonality (additive periodic components) in time-series using a Fourier basis in a overall feed-forward DL framework [20].

Our main contribution here involves a novel ED architecture for seasonal modelling using more than one encoder and incorporating multi-step (target) learning. The overall contribution summary is as follows:

- We propose a novel Encoder-Decoder based nonlinear SARX model which explicitly incorporates (stochastic) seasonal correlations. The framework can elegantly address multi-step (target) learning with exogenous inputs. It allows for multiple encoders depending on the order of seasonality. *The seasonal lag inputs are intelligently split between encoder and decoder inputs based on idea of the multiplicative seasonal AR model.*
- To utilize the above novel scheme for multiple sequence data, where per sequence data or variation in exogenous variables is less, we propose a novel greedy recursive procedure by grouping normalized sequences. The idea

* Avinash Achar is the corresponding author.

§ Both authors contributed equally.

Avinash Achar, & Soumen Pachal are with TCS Research, Chennai, INDIA.
E-mail: {*achar.avinash,s.pachal*}@tcs.com.

Manuscript received

is to build one or a few background models which can be used to predict for all sequences.

- We demonstrate effectiveness of the proposed architecture on real data sets involving both single and multiple sequences. Our experiments illustrate the proposed method's performance is competitive with state-of-art and outperforms some of the existing methods.

The paper overall is organized as follows. Sec. II discusses related work and puts the proposed work in perspective of current literature. Sec. III describes the proposed seasonal architecture for a single time-series. We next explain a novel recursive grouping algorithm in Sec. IV, which allows the proposed seasonal architecture to handle multiple sequence data. By bench-marking against various state-of-art baselines, we demonstrate the efficacy of our proposed architecture on both single and multiple sequence scenarios in Sec. V. We provide concluding remarks in Sec. VI.

II. Related Work

Times series forecasting has a long literature spanning more than five decades. Classical approaches include AR, MA, ARMA [15], exponential smoothing, linear state space models etc. A wide spectrum of non-linear approaches have also been explored over the years ranging from feed-forward networks, RNNs [10], [21], SVMs [22], random forests [23] and so on to the recent temporal convolutional networks (TCN) [24], with applications spanning across domains. These non-linear techniques have been shown to outperform the traditional techniques. The renewed surge in ANN research over the past decade has seen DL in particular being significantly explored in time series forecasting as well. For a review on deep networks for time series modelling, please refer to [25].

While traditionally time-series forecasting has focused on single time-series or a bunch of independent sequences, the problem of simultaneously forecasting a huge set of correlated time series is gaining traction given the increased availability of such data. Examples include demand forecasting of items in retail, price prediction of stocks, traffic state/congestion across signals, weather patterns across locations etc. There exist many recent sophisticated approaches tackling this high-dimensional problem [16]–[19], [26], [27]. Of these, [26], [27] adopt some variant of a matrix/tensor factorization (MF) approach on the multi-variate data. [19] employs CNN layers first (on the 2-D data) followed by RNN layers. [16]–[18] consider an RNN architecture at a single time-series level and extend it to multiple time series by essentially scaling sequences. Our proposed architecture is also at a single time-series level but different due to the seasonality feature. Our approach to handle multi-sequence learning also employs sequence-specific scaling but goes much beyond this, as described in Sec. IV.

A. Proposed architecture in perspective

Two uni-variate ED based attention variants and simple multivariate extensions of these (which do not look scalable to large number of sequences) is considered in [21]. [21] doesn't consider exogenous inputs in their architecture. To incorporate

seasonal correlations especially when period or cycle length is large, it would need a proportionately large input window width depending on order of seasonality. This would need a large proportionate set of additional parameters to be learnt which capture the position based attention feature of [21]. This can also lead to (i)processing irrelevant inputs which may not influence prediction (ii)vanishing gradient issue in spite of attention. While in our method, we consider multiple encoders where the k^{th} encoder captures the correlations from exactly k periods behind the current instant. *By picking the state from the last time-step of each of these encoders and concatenating them, there is equal emphasis/representation from each of the cycles towards the decoder input.* This is also unlike [21], where a convex combination of all states (of the single encoder) is the context vector. This may not retain information distinctly from each seasonal cycle for instance. Also, in our approach, since we split inputs across cycles into parallel encoders each of length much lesser compared to a single encoder, the vanishing gradient issue is potentially better mitigated.

[16] propose an ED architecture where targets are fed at decoder output, while exogenous inputs at prediction instants are fed as decoder inputs. *Our seasonal ED architecture can be viewed as a non-trivial generalization of this Seq2Seq architecture for multi-step prediction.* They also suggest certain improvements to the basic ED architecture for quicker learning etc. They also consider probabilistic (or interval forecasts) using quantile loss, which can be readily incorporated in our proposed architecture as well.

DeepAR [17] and DeepSS [18] use a many-to-many architecture with exogenous inputs (NARX model) for sales prediction of multiple amazon products). They don't consider stochastic seasonal correlations. During multi-step prediction, the prediction of the previous step is recursively fed as input to the next time-step, which means this strategy can lead to recursive error accumulation. Both methods also consider probabilistic forecasts by modelling network outputs as parameters of a negative binomial OR a linear dynamical system.

[19] propose LSTNet, another multiple time-series approach where a combination of CNN and RNN approaches are employed. The convolutional filters filter in only one dimension (namely time) across the 2-D input time-window to learn cross-correlations across sequences. The subsequent RNN part attempts to capture stochastic seasonal correlations via skip connections from a cycle (or period) behind. Applications where period is large results in unusually long input windows. While in our approach, we avoid skip connections and feed the seasonal lags from each cycle into a separate encoder (one or more depending on the order of seasonality).

N-Beats [20] considers a DL approach using feed-forward structures where deterministic periodicities (referred to seasonality as well in literature) are captured using Fourier basis. A signal in general can exhibit both kinds of seasonality: (i)deterministic periodic components (ii)stochastic seasonal correlations. A linear seasonal ARMA model for instance only captures stochastic seasonal correlations which is different from additive deterministic periodicity. Our seasonal ED architecture precisely captures such stochastic correlations making

it distinct from N-Beats.

Earlier described MF approaches though capture global features in the multi time-series setting, either do not (1)capture seasonality, (2)not allow for predictions with exogenous inputs or (3)learn with multi-step targets as in our approach. For details on MF methods, refer to appendix.

III. Proposed Seasonal ED Architecture

Sec. III-A and III-B respectively describe the motivation (from the linear multiplicative seasonal model) and actual proposed RNN architecture capturing a seasonal NARX model capable of multi-step prediction. Sec. IV describes a heuristic algorithm to adapt the proposed architecture for multiple sequence prediction.

Amongst three standard recurrent structure choices of plain RNN (without gating), LSTM [11] and GRU [28], we choose GRU in this paper. Like LSTM unit, GRU also has a gating mechanism to mitigate vanishing gradients and have more persistent memory. But lesser gate count in GRU keeps number of weight parameters much smaller. GRU unit as the building block for RNNs is currently ubiquitous across sequence prediction applications [29]–[32]. A single hidden layer plain RNN unit's hidden state would be

$$h_t = \sigma(W^h h_{t-1} + W^u u_t) \quad (1)$$

where W^h , W_u are the weight matrices associated with the state at the previous time-instant h_t and the current input ($u(t)$) respectively, $\sigma(\cdot)$ denotes sigma function. GRU based cell computes its hidden state (for one layer as follows)

$$z_t = \sigma(W^z u_t + U^z h_{t-1}) \quad (2)$$

$$r_t = \sigma(W^r u_t + U^r h_{t-1}) \quad (3)$$

$$\tilde{h}_t = \tanh(r_t \circ U h_{t-1} + W u_t) \quad (4)$$

$$h_t = z_t \circ h_t + (1 - z_t) \circ \tilde{h}_t \quad (5)$$

where z_t is update gate vector and r_t is the reset gate vector. If the two gates were absent, we essentially have the plain RNN. \tilde{h}_t is the new memory (summary of all inputs so far) which is a function of u_t and h_{t-1} , the previous hidden state. The reset signal controls the influence of the previous state on the new memory. The final current hidden state is a convex combination (controlled by z_t) of the new memory and the memory at the previous step, h_{t-1} . All associated weights W^z , W^r , W , U^z , U^r , U are trained using back-propagation through time (BPTT).

A. Motivation from multiplicative SAR model

The proposed *ED-based* multi-step, seasonal-NARX architecture can be motivated from the classical linear multiplicative SAR model as described in this section. A multiplicative seasonal AR model [33] is a stochastic process which satisfies the following equation.

$$(1 - \psi_1 L - \dots - \psi_p L^p)(1 - \Psi_1 L^S - \dots - \Psi_k L^{PS})y(t) = e(t). \quad (6)$$

where, $e(t)$ is a zero mean, white noise process with unknown variance, σ_e^2 . L^p is the one-step delay operator applied p times

i.e. $L^p y(t) = y(t - p)$. In a multiplicative SAR model (6), the auto-regressive term is a product of two lag polynomials: (a) first capturing standard lags of order up to p , (b) second capturing influence of seasonal lags at multiples of the period S and order up to P . Let us expand the associated product in eqn. (6) to obtain

$$\begin{aligned} y(t) = & a_1 y(t-1) + a_2 y(t-2) + \dots + a_p y(t-p) + b_0^1 y(t-S) \\ & + b_1^1 y(t-S-1) + \dots + b_p^1 y(t-S-p) + \dots \dots + \\ & b_0^P y(t-PS) + b_1^P y(t-PS-1) + \dots + \\ & b_p^P y(t-PS-p) + e(t) \end{aligned} \quad (7)$$

Note in the above equations p is assumed significantly less than S . Expanding out the product of the two polynomials in eqn. (6) and comparing it with eqn. (7), yields the following relations between the respective coefficients: $a_i = \psi_i$, $b_0^1 = \Psi_1$, $b_i^1 = -\psi_i \Psi_1$, $b_0^k = \Psi_k$, $b_i^k = -\psi_i \Psi_k$. *Observe from eqn. 7 that $y(t)$ is linearly auto-regressed w.r.t three types (categories) of inputs: (a) its p previous values ($y(t-1), y(t-2) \dots y(t-p)$) (b) values exactly a period S (or an integral multiple of S lags) behind, up to P cycles ($y(t-S), y(t-2S) \dots y(t-PS)$) (c) P groups of p consecutive values, where i^{th} such group is immediately previous to $y(t-iS)$, where $i = 1, 2, \dots P$. For instance, $y(t-iS-1), y(t-iS-2), \dots y(t-iS-p)$ is the i^{th} group of these P groups.*

We generalize the above structure of the expanded SAR model as follows. We first allow all co-efficients in eqn. (7) to be unconstrained. We further assume that the P groups of consecutive values (indicated in (c) above) need not be of the same size p . The below equation demonstrates this.

$$\begin{aligned} y(t) = & a_1 y(t-1) + \dots + a_p y(t-p) + b_0^1 y(t-S) \\ & + b_1^1 y(t-S-1) + \dots + b_{Q_1}^1 y(t-S-Q_1) + \dots \dots + \\ & b_0^P y(t-PS) + b_1^P y(t-PS-1) + \dots + \\ & b_{Q_P}^P y(t-PS-Q_P) + e(t) \end{aligned} \quad (8)$$

Please note that Q_i denotes the size of the i^{th} such group. The RNN structure we propose here adopts a nonlinear auto-regressive version of eqn. (8) given as follows.

$$\begin{aligned} y(t) = & F \left(\underbrace{y(t-1), y(t-2), \dots, y(t-p)}_{\text{category (a)}}, \right. \\ & \underbrace{y(t-S), y(t-2S), \dots, y(t-PS)}_{\text{category (b)}}, \\ & \underbrace{y(t-S-1), y(t-S-2), \dots, y(t-S-Q_1)}_{\text{category (c)}}, \\ & \underbrace{y(t-2S-1), y(t-2S-2), \dots, y(t-2S-Q_2), \dots}_{\text{category (c)}}, \\ & \left. \underbrace{y(t-PS-1), y(t-PS-2), \dots, y(t-PS-Q_P)}_{\text{category (c)}} \right) \end{aligned} \quad (9)$$

Note that the 3 categories above indicated by the 3 different styles of underlining correspond to the three categories ((a),(b),(c)) described earlier. *In the presence of an additional exogenous variable (process) $x(t)$, we additionally regress the endogenous variable $y(t)$ w.r.t to $x(t)$ at the current time t*

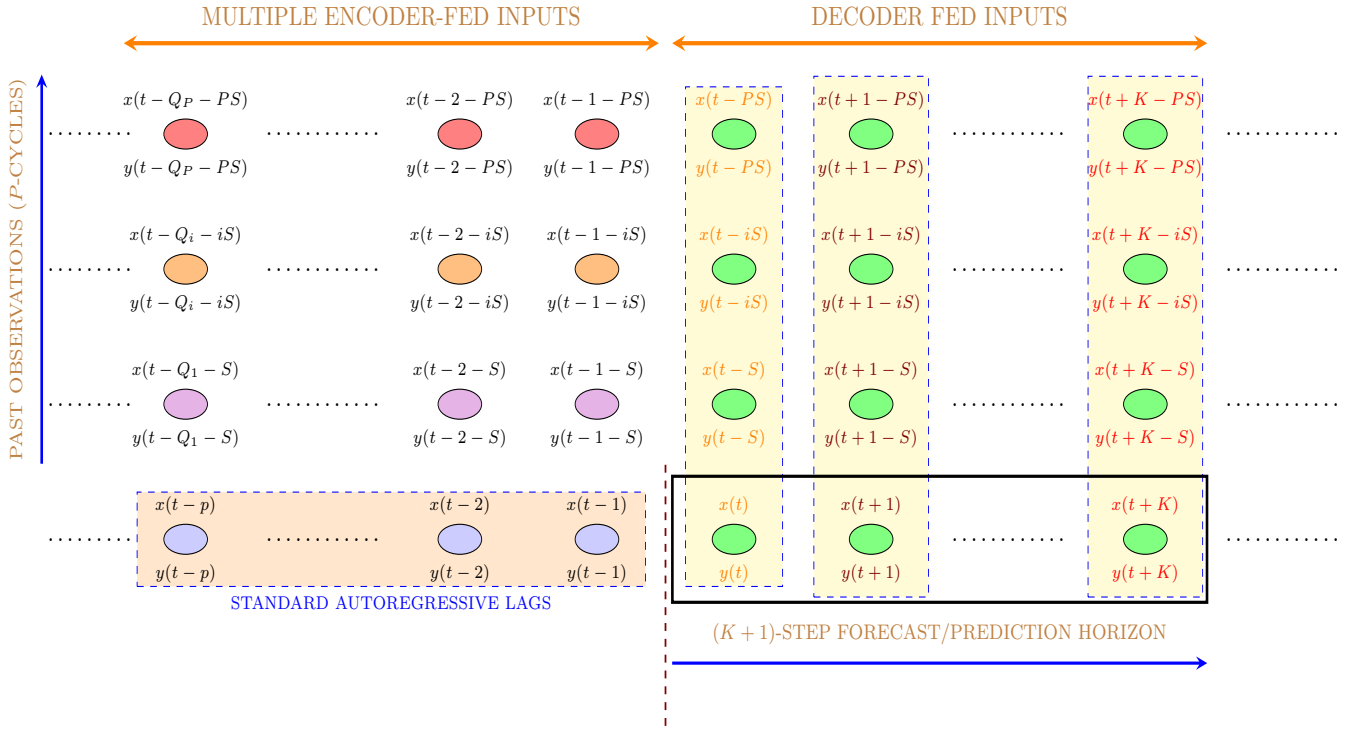


Fig. 1. Single sequence which starts from top left and ends on bottom right. Illustration of the Multi-step Seasonal NARX model input-outputs.

and all those previous time instants where $y(t)$ is exactly auto-regressed as per eqn. (8) as follows.

$$y(t) = F \left(\underbrace{x(t), x(t-1), y(t-1), \dots, x(t-p), y(t-p)}_{\text{Standard Autoregressive Lags}}, \underbrace{x(t-S), y(t-S), \dots, x(t-PS), y(t-PS)}_{\text{Seasonal Lags}}, \underbrace{x(t-S-1), y(t-S-1), \dots, y(t-S-Q_1)}_{\text{Lags}}, \underbrace{x(t-2S-1), y(t-2S-1), \dots, y(t-2S-Q_2)}_{\text{Lags}}, \dots, \underbrace{x(t-PS-1), y(t-PS-1), \dots, y(t-PS-Q_P)}_{\text{Lags}} \right) \quad (10)$$

The above model could be used for multi-step prediction by recursively computing single-step predictions sequentially. However, this can accumulate errors and lead to poor performance. Instead of predicting $y(t)$ alone, to predict $y(t)$ and $y(t+1)$ simultaneously, by the grammar of the multiplicative SARX model (given data till $t-1$), we potentially need *additional inputs* for prediction. Being a model with exogenous inputs, it definitely needs $x(t+1)$ additionally. Being a seasonal model, it would need additional inputs from lags which are one seasonal lag (or its multiples) behind $y(t+1)$. Specifically, it would need $x(t+1-S)$, $y(t+1-S)$, $x(t+1-2S)$, $y(t+1-2S)$, \dots , $x(t+1-PS)$, $y(t+1-PS)$. Generalizing this to a $K+1$ -step ahead one-shot predictive model, we obtain a model or map $F(\cdot)$ which predicts multi-step vector targets in presence of exogenous variables incorporating stochastic

seasonal correlations.

$$\begin{aligned} & \left(y(t), y(t+1), y(t+2), \dots, y(t+K) \right) = \\ & F \left(\underbrace{x(t), x(t+1), x(t+2), \dots, x(t+K)}_{\text{Future Exogenous Inputs}}, \underbrace{x(t-1), y(t-1), x(t-2), \dots, x(t-p), y(t-p)}_{\text{Standard Autoregressive Lags}}, \underbrace{x(t-S), y(t-S), \dots, x(t-PS), y(t-PS)}_{\text{Seasonal Lags}}, \underbrace{x(t+1-S), y(t+1-S), \dots, y(t+1-PS)}_{\text{Lags}}, \dots, \underbrace{x(t+K-S), y(t+K-S), \dots, y(t+K-PS)}_{\text{Lags}}, \underbrace{x(t-S-1), y(t-S-1), \dots, y(t-S-Q_1)}_{\text{Lags}}, \underbrace{x(t-2S-1), y(t-2S-1), \dots, y(t-2S-Q_2)}_{\text{Lags}}, \dots, \underbrace{x(t-PS-1), y(t-PS-1), \dots, y(t-PS-Q_P)}_{\text{Lags}} \right) \quad (11) \end{aligned}$$

For each additional component $y(t+i)$ in the target, there is an additional group of $2P$ inputs $x(t+i-S)$, $y(t+i-S)$, \dots , $x(t+i-PS)$, $y(t+i-PS)$ that need to be added as inputs. Since k varies from 0 to K , we have K such additional groups each of size of $2P$. These additional groups of inputs can all be viewed as belonging to a generalized category (b), introduced earlier. This is indicated by the additional groups of inputs introduced in eqn. (11) over eqn. (10). All these additional K groups are indicated using horizontal curly braces used earlier for inputs of category (b). Note that an additional category of the future exogenous inputs $x(t)$, $x(t+1)$, $x(t+2)$, \dots , $x(t+K)$ grouped with a dotted underline additionally appears in eqn. (11).

B. Encoder-Decoder RNN Architecture for Multi-step Seasonal NARX Model

To predict accurately during multi-step prediction, we train with vector-valued targets, the vector size equal to prediction horizon. The classical Seq2Seq (ED) can be neatly adapted to the multi-step context where the decoder is unfolded as much as the prediction horizon length ($K + 1$ steps).

Fig. 1 gives an example sequence shown in four rows, where the sequence starts from the top left and ends on the bottom right. It gives a pictorial view of the inputs utilized (up-to P cycles behind the current time t) for prediction from time t on-wards. Fig. 2 describes the associated proposed architecture with color coding of inputs and blocks matched with that of Fig. 1.

We implement eqn. (11) in an intelligent and non-redundant fashion using a novel ED architecture. We rewrite eqn. 11 by reorganizing its inputs as follows which aids us in clearly associating the inputs and outputs of the above multi-step seasonal NARX model to the proposed ED architecture.

$$\begin{aligned}
 & \left(y(t), y(t+1), y(t+2), \dots, y(t+k) \right) = \\
 & F \left(\underbrace{x(t-1), y(t-1), x(t-2), \dots, x(t-p), y(t-p)}_{\text{standard auto-regressive lags}}, \right. \\
 & \underbrace{x(t-S-1), y(t-S-1), \dots, x(t-S-Q_1), y(t-S-Q_1)}_{\text{seasonal lags } Q_1}, \\
 & \underbrace{x(t-2S-1), y(t-2S-1), \dots, y(t-2S-Q_2), \dots}_{\text{seasonal lags } Q_2}, \\
 & \underbrace{x(t-PS-1), y(t-PS-1), \dots, y(t-PS-Q_P)}_{\text{seasonal lags } Q_P}, \\
 & \underbrace{x(t), x(t-S), y(t-S), \dots, x(t-PS), y(t-PS)}_{\text{exogenous inputs}}, \\
 & \underbrace{x(t+1), x(t+1-S), y(t+1-S), \dots, y(t+1-PS), \dots}_{\text{exogenous inputs}}, \\
 & \left. \underbrace{x(t+K), x(t+K-S), y(t+K-S), \dots, y(t+K-PS)}_{\text{exogenous inputs}} \right) \quad (12)
 \end{aligned}$$

The finer splits in inputs in Fig. 1 are in sync with the input rearrangement of eqn. (12).

The first group in the rearrangement of eqn. (12) comes from standard immediate consecutive lags of order p . Note the lags shaded in blue and grouped as “standard auto-regressive” lags in Fig. 1. These inputs of category (a) are fed as input to Encoder 0 (GRU units shaded in blue). This is followed by P groups of seasonal lags, where the i^{th} such group is a bunch of Q_i consecutive lags starting exactly iS lags behind current time t . All time points in Fig. 1 above the “standard auto-regressive lags” represent these P groups. Each group here is colored differently and is fed into a separate encoder (Fig. 2) with GRU units colored in sync with the color of the associated time points in Fig. 1. In essence, we propose to have multiple encoders depending on the order P of the model. *This ensures that there is equal emphasis from seasonal lags of all orders during model building.* As observed, we also feed all the associated past exogenous inputs/observations at these various encoder time steps. *Context vectors obtained at the last time-step of each of these P encoders are appended before feeding further as initial state at the decoder’s first time-step.* To ensure better learning, the appended context vector can

also be additionally fed as an input at each time step of the decoder.

In addition, the ED framework can admit exogenous inputs during $(K + 1)$ -step forecast horizon as additional inputs at the respective time-steps of the decoder. Let us return to the rearrangement of inputs in eqn. (12) from eqn. (11). We observe that the future exogenous inputs $x(t), x(t+1), \dots, x(t+K)$ were distinctly present as the first group of inputs in eqn. (11). For each of these future exogenous inputs in eqn. (11), there exists a unique group of $2P$ past inputs/observations (endogenous + exogenous) $x(t+k-S), y(t+k-S), \dots, x(t+k-PS), y(t+k-PS)$, underlined with horizontal curly braces in eqn. (11). Eqn. (12) merges each $x(t+k), k = 0, 1, \dots, K$ with its uniquely associated group as just described above. Therefore we have $K + 1$ such groups of $2P + 1$ inputs. Each of these groups is indicated in Fig. 1 with a yellow shaded vertical grouping enclosed in blue dotted rectangles. The associated inputs of each group is color coded differently and the same color is carried forward in the decoder inputs of Fig. 2. Specifically, the k^{th} such group of $2P + 1$ inputs is fed as input to the k^{th} time-step of the decoder (Fig. 2). The $K + 1$ outputs in eqn. (11) are the targets at the $K + 1$ time-steps of the decoder output.

1) Seasonal lag distribution between encoder & decoder: Let us start with $P = 1$ case. To predict for $y(t)$, recall that the one-step endogenous model eqn. (8) needs as input $y(t-S)$ from exactly one cycle behind and Q_1 lags preceding it. A $(K + 1)$ -step ahead predictive model (eqn. 12 without exogenous inputs) from $y(t)$ to $y(t+K)$ would depend on data from $y(t-S)$ to $y(t-S+k)$ (exactly one cycle behind the prediction instants) and Q_1 lags preceding $y(t-S)$. *Hence, note that this block of Q_1 lags are invariant to the multi-step prediction horizon length. That’s why this block of lags is fed as a separate encoder. Its immediately succeeding lags are fed at the decoder end as they can be exactly matched (OR synchronized) with one of the multi-step targets exactly one period ahead.* That’s why we see data from time points $y(t-S)$ to $y(t-S+k)$ fed as decoder inputs from the first to the $(K + 1)^{\text{th}}$ time-step respectively. For $P > 1$, this kind of synchronized inputs at the decoder can additionally come from lags exactly $2S, \dots, PS$ time points behind. This means depending on P , each time step of the decoder receives input from P time points each of which are exactly iS steps behind, where $i = 1, \dots, P$.

Remark 1: *Overall the seasonal lag inputs are intelligently split between the encoder and decoder inputs avoiding any redundant inputs. Lags that influence all instants in the prediction horizon are fed via the encoders, while lags which are exactly a cycle (or its integral multiple) behind a point in the predictive horizon are fed at the decoder in a synchronous fashion. Even in the absence of exogenous inputs, the ED architecture proposed still holds with multiple encoders and the decoder inputs coming from the synchronized past observations of the endogenous variable.*

Remark 2: *We adopt a moving window approach in this paper and form a training example from every possible window in the time series. An example input-output window is best illustrated in Fig. 1.*

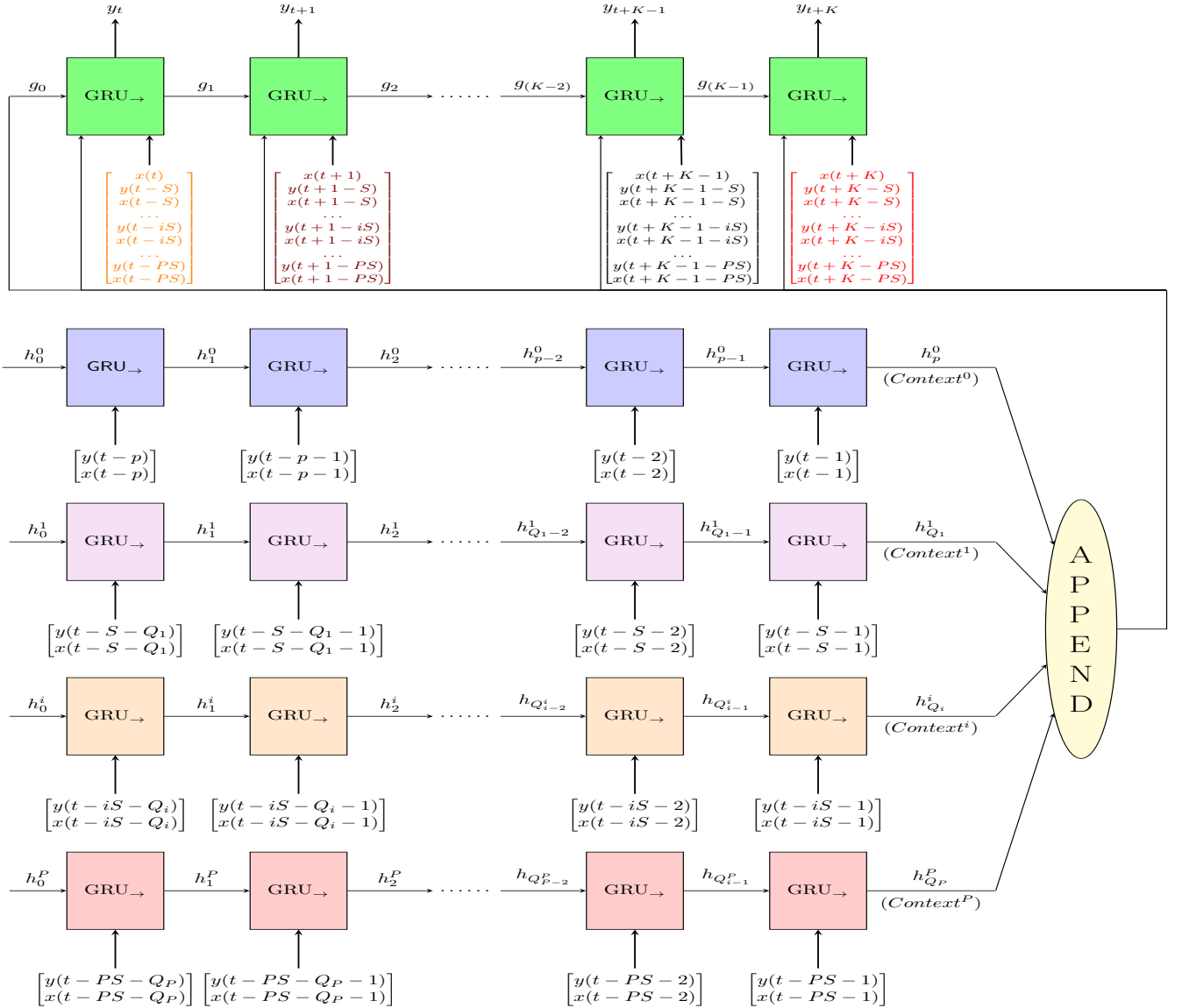


Fig. 2. Encoder-Decoder RNN based Seasonal Multi-step NARX Architecture

Algorithm 1: Build one or more background models to cover all sequences.

Input: Set of sequences \mathcal{T} .

Output: a set of models \mathcal{M} which cover all sequences.

- 1 Perform a sequence specific scaling (min-max normalization) of each sequence (time-series) T (both Y and X components of T) in \mathcal{T} .
- 2 Initialize $\mathcal{G} \leftarrow \mathcal{T}$.
- 3 *Model-Recursive-fn*(\mathcal{G});

IV. Training and prediction on multiple sequences

While the proposed architecture can be used for a single time series case, using it for multiple time-series prediction is not clear. To be able to adapt our architectures for prediction across *short length* multiple time-series, we present a novel greedy recursive algorithm. The overall idea of this algorithm is that there exist one or at most a handful of models which

explain all the sequences in a scaled (or normalized) domain. This can be employed in situations where building RNN models per sequence is infeasible due to data scarcity at a sequence level. This could be very useful in situations where the variations in the exogenous variable is also little for every sequence.

Alg. 1 together with Alg. 2 explains the overall procedure. Line 1 performs a seq-specific scaling of the both the Y (endogenous) and X (exogenous) components as an attempt to build common models in the normalized domain. The set of scaled sequences are now fed to the recursive function *Model-Recursive-fn*(.) (given in Alg. 2). Build a model using all sequences in \mathcal{G} which can predict for all sequences T in \mathcal{G} (line 2). We evaluate the model performance sequence-wise for every $T \in \mathcal{G}$ (based on a separate validation set). The error metrics could be MASE or MAPE for instance (refer to the next section for details). We keep aside all sequences $T \in \mathcal{G}$ on which the model M 's (validation) error ($e(T)$) is below a user-defined threshold (E_{th}) into \mathcal{G}_1 (line 4). If \mathcal{G}_1 is empty

Algorithm 2: Model-Recursive-fn(\mathcal{G})

Input: \mathcal{G} (subset of sequences from \mathcal{T})

- 1 Form training examples from all the sequences in \mathcal{G} ;
- 2 Build one RNN model M using the above possible examples, which can predict for all $T \in \mathcal{G}$. (M predicts for all sequences in the normalized domain). ;
- 3 Apply inverse sequence specific scaling for each sequence to evaluate sequence specific prediction errors;
- 4 Form $\mathcal{G}_1 := \{T \in \mathcal{G} : e(T) \leq E_{th}\}$;
- 5 **if** $\mathcal{G}_1 \neq \phi$ **then**
- 6 Add (M, \mathcal{G}_1) to \mathcal{M} ;
- 7 Form $\mathcal{G}_2 \leftarrow \mathcal{G} \setminus \mathcal{G}_1$;
- 8 **if** $\mathcal{G}_2 == \phi$ **then**
- 9 return;
- 10 **else**
- 11 *Model-Recursive-fn*(\mathcal{G}_2);
- 12 **else**
- 13 We build sequence specific models to all sequences in \mathcal{G} ;
- 14 Add all these models to \mathcal{M} ;
- 15 return;

(line 12), then we build sequence specific models using linear time series OR shallow RNN models (line 13–15) and return. If \mathcal{G}_1 is non-empty (line 5), we first add the current model M and the current set of sequences \mathcal{G}_1 to \mathcal{M} (line 6). While its compliment in \mathcal{G} , namely \mathcal{G}_2 (line 7) is also non-empty (line 10), we attempt to build an additional model greedily on \mathcal{G}_2 (set of sequences on which the current model M performs poorly), as per line 11. If \mathcal{G}_2 is empty, we return (line 9).

V. Results

We first describe the data sets used for testing, followed by error metrics and hyper-parameters for evaluation, and performance results in comparison to some strong base lines.

A. Data Sets

- **D1:** This is demand data from National Electricity Market of Australia. Australian geography is split into 5 disjoint regions, which means we have five power demand time series including an aggregate temperature time-series (exogenous input) in each of these regions. This is a single time-series data-set consisting of 5 independent time-series. D1 is 3 months of summer data (Dec to Feb) from these 5 regions. The granularity of the time-series here is half-hourly. The last 2 weeks were used for testing.
- **D2:** M5 data-set¹ is a publicly available data-set from Walmart and contains the unit sales of different products on a daily basis spanning 5.4 years. This data is distributed across 12 different aggregation levels. Amongst these levels, aggregation level 8 contains unit sales of all products, aggregated for each store and category. Price is used as exogenous input here. *This level contains 30 sequences. Based on the PACF value at the 365th*

($S=365$) lag, we choose top 3 sequences, which we refer to as D2. We focus on sequences which have significant PACF based evidence of stochastic seasonal correlations.

- **D3:** This is publicly available from Walmart². The measurements are weekly sales at a department level of multiple departments across 45 Walmart stores. In addition to sales, there are other related measurements like CPI (consumer price index), mark-down price etc. which we use as exogenous variables for weekly sales prediction. The data is collected across 3 years and its a multiple time-series data. The whole data set consists of 2628 sequences. For purposes of this paper, *we ranked sequences based on total variation of the sales and considered the top 20% of the sequences (denoted as D3) for testing.* We essentially pick the hardest sequences which exhibit sufficient variation. The total variation of a T length sequence x is defined as

$$TV = \sum_{i=2}^T |(x(i+1) - x(i))| \quad (13)$$

- **D4:** Data at level 10 from M5 data-set(described above) contains unit sales product-wise aggregated for all store/states. This level contains a total of 3049 sequences as there are that many products. In order to simulate a situation where per sequence data is relatively less, we consider only last 3 years data at a weekly resolution (instead of daily) by further aggregating sale units across a week. A single price is the exogenous variable here. Further we ranked the 3049 sequences based on total variation and considered the top 20% of these sequences (similar to D3), which we refer to as D4 (containing 609 sequences in total). D4, product level data (level 10 - M5) has characteristics different from D3 (Walmart), which is department level sales (aggregated across products).

B. Error metrics and Hyper-parameter choices

We consider the following two error metrics: (1)**MAPE** (Mean Absolute Percentage Error) (2)**MASE** (Mean Absolute Scale Error [34])

The APE is essentially relative error (RE) expressed in percentage. If \hat{X} is predicted value, while X is the true value, the RE = $(\hat{X} - X)/X$. In the current multi-step setting, APE is computed for each step and is averaged over all steps to obtain the MAPE for one window of the prediction horizon. The APE while has the advantage of being a scale independent metric, can assume abnormally high values and can be misleading when the true value is very low. An alternative complementary error metric which is scale-free could be MASE.

The MASE is computed with reference to a baseline metric. The choice of baseline is typically the copy previous predictor, which just replicates the previous observed value as the prediction for the next step. For a given window of one prediction horizon of K steps ahead, let us denote the i^{th} step error by $|\hat{X}_i - X_i|$. The i^{th} scaled error is defined as

$$e_s^i = \frac{|\hat{X}_i - X_i|}{\frac{1}{n-K} \sum_{j=K+1}^n |X_j - X_{j-K}|} \quad (14)$$

¹<https://www.kaggle.com/c/m5-forecasting-accuracy/data>

²<https://www.kaggle.com/c/walmart-recruiting-store-sales-forecasting/data>

where n is no. of points in the training set. The normalizing factor is essentially the average i^{th} step-ahead error of the copy-previous baseline on the training set. Hence MASE on a multi-step prediction window w of size K will be

$$MASE(w, K) = \frac{1}{K} \sum_{j=1}^K e_s^j \quad (15)$$

1) **Hyper-parameters:** Tab. I describes the broad choice of hyper-parameters during training in our experiments.

TABLE I
MODEL PARAMETERS FOR DURING TRAINING.

Parameters	Description
Batch size	256/64
Learning Rate	0.002
No. of Epochs	40/70
Number of Hidden layers	1/2
Hidden vector dimensionality	7/17
Optimizer	RMSProp

C. Baselines

We denote our seasonal approach compactly by SEDX. We focused on base-lining against traditional time-series and state-of-art RNN approaches. We didn't consider non-RNN DL approaches like N-Beats, Temporal Convolutional Networks etc. whose underlying architectures are a bit different. The baselines we benchmark our method against are as follows:

- 1) SARX - Seasonal AR with exogenous inputs (strong standard linear time-series baseline). We stick to an AR model here as a sufficiently long AR model can approximate any ARMA model in general. For D1, D2 the AR orders are also determined from PACF. Given half-an-hour granularity of the data, we choose $S = 48$ to capture daily seasonality in D1. In D2, which is daily data, we choose $S = 365$ to capture yearly seasonality. For D3, D4 we read off the sequence-specific orders p from the respective PACFs, $S = 52$ to capture yearly seasonality. For D3 and D4, we choose $P = 1$ (eqn. 6) not only for SARX, but all the other non-linear baselines, as we have only about 3 years of data per sequence.
- 2) BEDX - Basic Encoder Decoder (with only one encoder capturing the immediate lags), while the exogenous inputs of the prediction instants are fed as inputs to the decoder as considered in [16]. It is a simplified SEDX with all structures and inputs from the seasonal lags excluded.
- 3) DeepAR [17] - explained earlier in Sec. II-A. We use a squared error loss for training which is equivalent to a Gaussian conditional log-likelihood of the targets (with a constant variance). The input window length is chosen consistent with that of SEDX.
- 4) LSTNet [19] - explained earlier in Sec. II-A. Other parameters include history length = 60, No of filters = 16, AR window size = 14, skip length = 52, dropout rate = 0.3.
- 5) PSATT [21] - explained earlier in Sec. II-A. We only consider the first variant of position-based attention

where each state component is weighted same. The second variant involving state component dependent weights can lead to too many extra parameters. Its multivariate extension does not scale well for large dimensions due to increased number of parameters to be learnt. In particular, data-sets D3 and D4 have a few hundred sequences (hence a high input dimension), while the per-sequence length is limited. Hence we do not consider PSATT for bench-marking on D3, D4. For D1 & D2, input window length is chosen to accommodate up-to PS lags.

In both D1 and D2, we didn't observe any evidence for integrating type non-stationarity in the ACF plots for instance. Typically, a very slow decay in the ACF is indicative of a possible integrating type non-stationarity in the data. Similarly a slow decay at the seasonal lags is indicative of a need for seasonal differencing to cancel the random walk non-stationarity.

1) **Assessing significance of mean error differences statistically:** We have conducted a Welch t-test (unequal variance) based significance assessment (across all relevant experiments) under both the mean metric (MASE, MAPE) differences (SEDX vs Baseline) with a significance level of 0.05 for null hypothesis rejection. In all subsequent tables, a simple way to indicate the best performing method is to highlight in bold the best/least MASE/MAPE. Our test of significance can strengthen this visualization by allowing for MASE/MAPE highlighting of other methods (multiple) whose mean error difference with the best method's MASE/MAPE (need not be SEDX always) is statistically insignificant. We test significance of mean differences when averaged at the (finest) test example level.

D. Results on Single-Sequence Data-sets (D1,D2)

1) **Results on D1:** For D1, the multi-step horizon was chosen to be 48 to be able to predict a day ahead (each time point is half-hourly demand). *There was evidence for seasonal correlations in the ACF in terms of local maxima at lags 48 and 96, which prompted us to choose $S = 48$ and seasonal order ($P = 2$).* To choose the length of the associated encoders, we look to the significant PACF values just behind the 48th and 96th lags. Tab. II indicates the error metrics in comparison to 4 feasible baselines (LSTNet is not applicable for the single sequence case). Our results demonstrate superior performance of SEDX against improvements of up to 1.94 in MASE and 34% in MAPE. In particular, SEDX outperforms SARX. Our significance analysis reveals SEDX's MASE/MAPE reduction compared to BEDX (in spite of visually close MAPEs) is actually statistically significant for R1 to R4.

TABLE II
(MASE, MAPE) ACROSS FIVE REGIONS IN AUSTRALIA

Region	SEDX	SARX	BEDX	DeepAR	PSATT
R1	(0.38,6)	(0.86,15)	(0.58,8)	(1.32,16)	(0.98,14)
R2	(0.37,4)	(0.41,5)	(0.46,5)	(1.18,18)	(1.09,11)
R3	(0.64,4)	(1.00,8)	(0.69,5)	(1.32,9)	(0.87,5.85)
R4	(0.71,10)	(1.58,24)	(0.73,11)	(1.48,18)	(1.11,15.22)
R5	(0.58,11)	(1.10,21)	(0.55,10)	(2.52,45)	(0.91,15.97)

2) **Results on D2:** For D2, the prediction horizon was set to be 28 days ($K = 28$). A test size of 33 days (time-points) was set aside for each sequence in D2. This means we tested for 6 windows of width 28 on the 33 day test set per sequence. Here we choose the seasonal order $P = 1$ with $S = 365$ (yearly seasonality is exploited) by analyzing ACF values. Tab. III gives the detailed comparison with all the 4 (single sequence) strong baselines in terms of both the error metrics. Our results demonstrate that SEDX mostly outperforms all 4 baselines on all 3 sequences, except for BEDX doing equally well (in a statistical sense) on seq 3. In particular, we observe improvements of up to 1.09 in MASE and 17.4% in MAPE in favor of our method.

TABLE III
(MASE,MAPE) ACROSS 3 SEQUENCES IN D2

Seq	SEDX	BEDX	DeepAR	SARX	PSATT
1	(0.62,10)	(0.77,11.8)	(1.39,22.2)	(1.15,17.8)	(1.71,27.4)
2	(0.69,9.9)	(0.82,11.8)	(1.11,16.2)	(0.88,12.2)	(0.99,13.9)
3	(0.69,11.1)	(0.76,11.7)	(1.52,23.2)	(0.91,14)	(0.95,14.1)

E. Results on Multiple-Sequence Data-sets (D3,D4)

1) **Results on D3:** We first demonstrate the effectiveness of SEDX on D3. A test size of 15 weeks (time-points) was set aside for each sequence in D3. We choose $K = 10$ time-steps in the decoder for training which means we tested for 6 windows of width 10 on the 15 week test set per sequence. For both D3 and D4, we append all sequences (normalized using sequence-specific normalization) into one long sequence and look at its Partial auto-correlation function (PACF). This enables us to fix the number of time-steps in the encoders corresponding to the seasonal correlations, which is typically much lesser than the number of time-steps in encoder 1 (which captures standard lags). On D3, with MASE based threshold (E_{th}) of 0.3, *Model-Recursive-fn()* ran for 2 rounds.

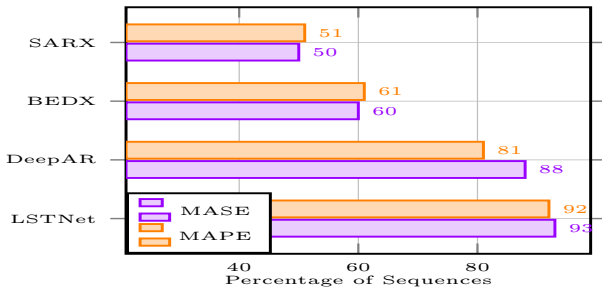


Fig. 3. Percentage of Sequences where SEDX does better

TABLE IV
MAX, AVG & MIN OF MASE & MAPE ACROSS ALL SEQUENCES

Method	MASE based			MAPE based in %		
	Max	Avg	Min	Max	Avg	Min
SEDX	2.75	0.54	0.16	76	13	2
SARX	2.38	0.56	0.11	69	14	2
BEDX	2.45	0.65	0.13	265	19	2
DeepAR	7.58	1.32	0.27	278	28	3
LSTNet	5.48	1.39	0.24	156	32	3

Fig. 3 gives a detailed breakup of percentage of sequences on which SEDX did better compared to the 4 baselines. It demonstrates *SEDX does better on at least 50% and up to 80% of the sequences compared to all considered baselines.*

Tab. IV gives average, max and min across sequences (of MASE and MAPE) for all methods. It demonstrates that on an average SEDX does better than all baselines based on both complementary metrics. *MASE improvements are up to 0.85 while the MAPE improvements are up to 19%.* Min and max were provided in Tab. IV (and Tab. VII) to honestly gauge error spread limits across sequences in D3 and D4. Viewing them as metric can be misleading.

On D3, SEDX performance might appear similar to SARX. But note from Fig. 3 and Tab. IV, that SEDX is actually complementing SARX on the 526 sequences of D1. SEDX is doing better than SARX on 50% of the sequences and giving a statistically significant improvement of 0.2(MASE) and 6% (MAPE) on sequences where SEDX does better (Tab. V,VI).

Tab. V looks at the (conditional) average MASE under two conditions with respect to each baseline: (i)average over those sequences on which SEDX fares better, (ii)average over those sequences on which the baseline does better. At this level, MASE improvements of at least 0.20 while up to 0.93 are observed. Tab. VI considers a similar (conditional) average MAPE. At this level of MAPE, there are improvements of at least 6% to up to 20%.

TABLE V
AVG MASE WHEN (I)SEDX IS BETTER (II)BASELINE IS BETTER.

Method	SEDX better			Baseline better		
	SEDX	BLine	Diff	SEDX	BLine	Diff
SARX	0.47	0.67	0.20	0.61	0.46	0.15
BEDX	0.49	0.79	0.30	0.62	0.44	0.18
DeepAR	0.50	1.40	0.90	0.86	0.65	0.21
LSTNet	0.51	1.44	0.93	0.98	0.70	0.28

TABLE VI
AVG MAPE WHEN (I)SEDX IS BETTER (II)BASELINE IS BETTER.

Method	SEDX better			Baseline better		
	SEDX	BLine	Diff	SEDX	BLine	Diff
SARX	10	16	6	18	13	5
BEDX	11	24	13	18	12	6
DeepAR	13	32	19	17	12	5
LSTNet	14	34	20	18	14	4

2) **Results on D4:** For D4, where data is at a weekly granularity a prediction horizon of 8 weeks ($K = 8$) was chosen for training while the chosen test size was 11 weeks for each sequence. This means for each sequence there are 4 (input-output) windows of output window width 8 on which we test. We chose a yearly seasonality here (with $S = 52$) similar to D3. On D4, with MASE based threshold (E_{th}) of 0.3, *Model-Recursive-fn()* ran for 1 round.

In this experiment, we observe a considerable fraction of sequences, where each of the 5 methods (proposed + 4 baselines) exhibit either high MASE or high MAPE. To quantify how high is unacceptable, we consider an MASE threshold of 1 (beyond which a naive copy previous predictor would be better) and MAPE threshold of 30%. For these thresholds,

we find 143 sequences on which each of the methods either have an MASE > 1 or MAPE > 30%. We have excluded such sequences because neither our method nor any of the proposed baselines perform within acceptable limits on these. For such sequences, one can potentially explore simpler baselines like copy previous predictor or ARX model (without seasonality). We demonstrate results on the remaining 466 sequences where at least one of the 5 methods (models) have both MASE < 1 and MAPE < 30%.

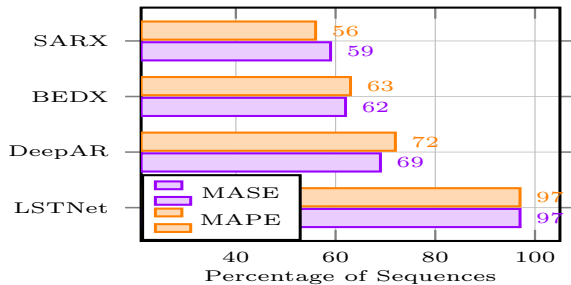


Fig. 4. Percentage of Sequences when SEDX does better(pictorially)

Fig. 4 represents the percentage of (the 466) sequences on which SEDX is better compared to all four baselines in terms of both the metrics. It shows that SEDX does better on at-least 59%(56%) of the sequences and up-to 97%(97%) in terms of MASE(MAPE), compared to all baselines.

TABLE VII
MAX, AVG AND MIN OF MASE AND MAPE ACROSS ALL SEQUENCES

Method	MASE based			MAPE based in %		
	Max	Avg	Min	Max	Avg	Min
SEDX	6.45	0.75	0.01	81.35	15.42	3.57
SARX	3.12	0.68	0.16	76.15	16.48	4.44
BEDX	6.78	0.83	0.01	99.36	17.29	3.51
DeepAR	6.62	0.91	0.02	88.22	19.74	2.97
LSTNet	17.29	1.78	0.02	307.54	35.08	6.20

Tab. VII gives the average, max and min of MASE and MAPE across the (466) sequences for all the models. It shows that on an average SEDX is better than all considered baselines in terms of MAPE while SARX does better in terms of MASE.

TABLE VIII
AVERAGE MASE WHEN (I)SEDX IS BETTER (II)BASELINE IS BETTER.

Method	SEDX better			Baseline better		
	SEDX	BLine	Diff	SEDX	BLine	Diff
SARX	0.37	0.78	0.41	1.31	0.54	0.77
BEDX	0.73	0.92	0.19	0.79	0.68	0.11
DeepAR	0.69	1.00	0.31	0.89	0.71	0.18
LSTNet	0.75	1.81	1.06	1.01	0.89	0.12

Tab. VIII represents the average MASE under two conditions: (i) sequences where SEDX does better (ii) sequences where baseline does better. It shows that MASE improvement of our proposed method is at-least 0.19 and up-to 1.06.

Tab. IX also represents similar conditions based on MAPE. There are MAPE improvement of at-least 4.18% and up-to 20.41%. Note that based on MAPE, the average conditional improvement (indicated as Diff) of SEDX when it does better (left half of the table) is uniformly better than the average

TABLE IX
AVERAGE MAPE WHEN (I)SEDX IS BETTER (II)BASELINE IS BETTER.

Method	SEDX better			Baseline better		
	SEDX	BLine	Diff	SEDX	BLine	Diff
SARX	12.83	18.40	5.57	18.69	14.06	4.63
BEDX	15.04	19.22	4.18	16.06	14.05	2.01
DeepAR	15.15	22.43	7.28	16.11	12.77	3.34
LSTNet	15.09	35.50	20.41	25.98	21.51	4.47

conditional improvements of all other baselines (Diff column on the right half of the table).

On D4, SEDX performance (over SARX) is actually better than in D3. Even though overall MASE avg of 0.68 (not MAPE please note) across all sequences looks better for SARX (Tab. VII), its only better on 41% of sequences in D4 (Fig. 4). Tab. IX indicates SEDX achieves a statistically significant improvement of 5.57% (over SARX) on 56% of sequences.

VI. Conclusions

We proposed a novel ED architecture for forecasting with multi-step (target) learning feature and prediction ability. The architecture generalized a linear multiplicative Seasonal ARX model using multiple encoders, each of which capture correlations from one or more cycles behind the prediction instant. The seasonal inputs were intelligently split between encoder and decoder without redundancy. We also proposed a greedy recursive grouping algorithm to build background predictive models (one or at most a few) for the multiple time series problem. We tested the proposed architecture and grouping algorithm on multiple real data sets, where our proposed architecture did mostly better than all strong baselines while it outperformed many of them. As future work, we would like to investigate how the proposed architecture could be utilized to better capture cross-sequence effects for multi time-series prediction. We reckon that the proposed architecture can be potentially useful in many more real world scenarios.

REFERENCES

- [1] A. van den Oord, S. Dieleman, H. Zen, K. Simonyan, O. Vinyals, A. Graves, N. Kalchbrenner, A. W. Senior, and K. Kavukcuoglu, "Wavenet: A generative model for raw audio," *CoRR*, vol. abs/1609.03499, 2016. [Online]. Available: <http://arxiv.org/abs/1609.03499>
- [2] F. Wang and D. M. J. Tax, "Survey on the attention based RNN model and its applications in computer vision," *CoRR*, vol. abs/1601.06823, 2016. [Online]. Available: <http://arxiv.org/abs/1601.06823>
- [3] A. Graves, M. Liwicki, S. Fernández, R. Bertolami, H. Bunke, and J. Schmidhuber, "A novel connectionist system for unconstrained handwriting recognition," *IEEE Trans. Pattern Anal. Mach. Intell.*, vol. 31, no. 5, pp. 855–868, May 2009.
- [4] A. Graves, A. Mohamed, and G. Hinton, "Speech recognition with deep recurrent neural networks," in *2013 IEEE International Conference on Acoustics, Speech and Signal Processing*, 2013, pp. 6645–6649.
- [5] A. Graves and N. Jaitly, "Towards end-to-end speech recognition with recurrent neural networks," in *Proceedings of the 31st International Conference on International Conference on Machine Learning - Volume 32*, 2014, pp. 1764–1772.
- [6] K. Cho, B. van Merriënboer, C. Gulcehre, D. Bahdanau, F. Bougares, H. Schwenk, and Y. Bengio, "Learning phrase representations using RNN encoder–decoder for statistical machine translation," in *Proceedings of the 2014 Conference on Empirical Methods in Natural Language Processing (EMNLP)*, Oct. 2014, pp. 1724–1734.

- [7] I. Sutskever, O. Vinyals, and Q. V. Le, "Sequence to sequence learning with neural networks," in *Proceedings of the 27th International Conference on Neural Information Processing Systems - Volume 2*, 2014, pp. 3104–3112.
- [8] R. Kiros, R. Salakhutdinov, and R. S. Zemel, "Unifying visual-semantic embeddings with multimodal neural language models," *CoRR*, vol. abs/1411.2539, 2014. [Online]. Available: <http://arxiv.org/abs/1411.2539>
- [9] K. Xu, J. L. Ba, R. Kiros, K. Cho, A. Courville, R. Salakhutdinov, R. S. Zemel, and Y. Bengio, "Show, attend and tell: Neural image caption generation with visual attention," in *Proceedings of the 32nd International Conference on Machine Learning - Volume 37*, 2015, pp. 2048–2057.
- [10] J. Connor, L. E. Atlas, and D. R. Martin, "Recurrent networks and narma modeling," in *Proceedings of the 4th International Conference on Neural Information Processing Systems*, 1991, pp. 301–308.
- [11] S. Hochreiter and J. Schmidhuber, "Long short-term memory," *Neural Comput.*, vol. 9, no. 8, pp. 1735–1780, Nov. 1997.
- [12] F. A. Gers, J. A. Schmidhuber, and F. A. Cummins, "Learning to forget: Continual prediction with lstm," *Neural Comput.*, vol. 12, no. 10, pp. 2451–2471, Oct. 2000.
- [13] F. M. Bianchi, E. Maiorino, M. C. Kampffmeyer, A. Rizzi, and R. Jenssen, "An overview and comparative analysis of recurrent neural networks for short term load forecasting," *CoRR*, vol. abs/1705.04378, 2017. [Online]. Available: <http://arxiv.org/abs/1705.04378>
- [14] L. Lu, X. Zhang, K. Cho, and S. Renals, "A study of the recurrent neural network encoder-decoder for large vocabulary speech recognition," in *Proceedings of the 16th Annual Conference of the International Speech Communication Association, INTERSPEECH*, Jan. 2015, pp. 3249–3253.
- [15] G. E. P. Box and G. Jenkins, *Time Series Analysis, Forecasting and Control*. Holden-Day, Incorporated, 1990.
- [16] R. Wen, K. Torkkola, B. Narayanaswamy, and D. Madeka, "A multi-horizon quantile recurrent forecaster," in *The 31st Conference on Neural Information Processing Systems (NIPS 2017), Time Series Workshop*, 2017.
- [17] D. Salinas, V. Flunkert, J. Gasthaus, and T. Januschowski, "Deepar: Probabilistic forecasting with autoregressive recurrent networks," *International Journal of Forecasting*, vol. 36, no. 3, pp. 1181–1191, 2020. [Online]. Available: <https://www.sciencedirect.com/science/article/pii/S0169207019301888>
- [18] S. S. Rangapuram, M. Seeger, J. Gasthaus, L. Stella, Y. Wang, and T. Januschowski, "Deep state space models for time series forecasting," in *Proceedings of the 32nd International Conference on Neural Information Processing Systems*, ser. NIPS'18, 2018, pp. 7796–7805.
- [19] G. Lai, W.-C. Chang, Y. Yang, and H. Liu, "Modeling long- and short-term temporal patterns with deep neural networks," in *The 41st International ACM SIGIR Conference on Research & Development in Information Retrieval*. New York, NY, USA: Association for Computing Machinery, 2018, pp. 95–104.
- [20] B. N. Oreshkin, D. Carpo, N. Chapados, and Y. Bengio, "N-beats: Neural basis expansion analysis for interpretable time series forecasting," in *International Conference on Learning Representations*, 2020. [Online]. Available: <https://openreview.net/forum?id=r1ecqn4YwB>
- [21] Y. G. Cinar, H. Mirisaee, P. Goswami, É. Gaussier, A. Ait-Bachir, and V. V. Strijov, "Position-based content attention for time series forecasting with sequence-to-sequence rnns," in *Neural Information Processing - 24th International Conference, ICONIP 2017*, ser. Lecture Notes in Computer Science, vol. 10638. Springer, 2017, pp. 533–544.
- [22] N. I. Sapankevych and R. Sankar, "Time series prediction using support vector machines: A survey," *IEEE Computational Intelligence Magazine*, vol. 4, no. 2, pp. 24–38, 2009.
- [23] M. Kane, N. Price, M. Scotch, and P. Rabinowitz, "Comparison of arima and random forest time series models for prediction of avian influenza h5n1 outbreaks," *BMC Bioinformatics*, vol. 15, no. 1, Aug. 2014.
- [24] A. Borovykh, S. Bohte, and C. W. Oosterlee, "Conditional time series forecasting with convolutional neural networks," 2018.
- [25] M. Långkvist, L. Karlsson, and A. Loutfi, "A review of unsupervised feature learning and deep learning for time-series modeling," *Pattern Recognition Letters*, pp. 11–24, 2014.
- [26] R. Sen, H. Yu, and I. S. Dhillon, "Think globally, act locally: A deep neural network approach to high-dimensional time series forecasting," in *Advances in Neural Information Processing Systems 32: Annual Conference on Neural Information Processing Systems 2019, NeurIPS 2019, December 8-14, 2019, Vancouver, BC, Canada*, 2019, pp. 4838–4847.
- [27] H.-F. Yu, N. Rao, and I. S. Dhillon, "Temporal regularized matrix factorization for high-dimensional time series prediction," in *Proceedings of the 30th International Conference on Neural Information Processing Systems*, ser. NIPS'16. Curran Associates Inc., 2016, pp. 847–855.
- [28] J. Chung, C. Gulcehre, K. Cho, and Y. Bengio, "Empirical evaluation of gated recurrent neural networks on sequence modeling," in *NIPS 2014 Deep Learning and Representation Learning Workshop*, 2014. [Online]. Available: <http://arxiv.org/abs/1412.3555>
- [29] A. Gupta, G. Gurrala, and P. S. Sastry, "Instability prediction in power systems using recurrent neural networks," in *Proceedings of the 26th International Joint Conference on Artificial Intelligence*. AAAI Press, 2017, pp. 1795–1801.
- [30] M. Ravanelli, P. Brakel, M. Omologo, and Y. Bengio, "Light gated recurrent units for speech recognition," *IEEE Transactions on Emerging Topics in Computational Intelligence*, vol. 2, no. 2, pp. 92–102, Apr 2018.
- [31] Z. Che, S. Purushotham, K. Cho, D. Sontag, and Y. Liu, "Recurrent neural networks for multivariate time series with missing values," *Scientific Reports*, vol. 8, Jun 2016.
- [32] N. Gruber and A. Jockisch, "Are gru cells more specific and lstm cells more sensitive in motive classification of text?" *Front. Artif. Intell.*, 2020.
- [33] P. Brockwell and R. Davis, *Introduction to time series and forecasting*. Springer, 2016.
- [34] R. J. Hyndman and A. B. Koehler, "Another look at measures of forecast accuracy," *International Journal of Forecasting*, vol. 22, no. 4, pp. 679–688, 2006.
- [35] Y. Koren, R. Bell, and C. Volinsky, "Matrix factorization techniques for recommender systems," *Computer*, vol. 42, no. 8, pp. 30–37, Aug. 2009.
- [36] L. Xiong, X. Chen, T.-K. Huang, J. Schneider, and J. G. Carbonell, "Temporal collaborative filtering with bayesian probabilistic tensor factorization," in *Proceedings of the 2010 SIAM International Conference on Data Mining*. SIAM, 2010, pp. 211–222.
- [37] S. Rallapalli, L. Qiu, Y. Zhang, and Y.-C. Chen, "Exploiting temporal stability and low-rank structure for localization in mobile networks," in *Proceedings of the Sixteenth Annual International Conference on Mobile Computing and Networking*, ser. MobiCom '10. New York, NY, USA: Association for Computing Machinery, 2010, pp. 161–172.

APPENDIX A MATRIX FACTORIZATION APPROACHES

Matrix factorization methods have been another class of methods to analyze multiple time series. Traditionally used for recommendation systems [35], they have also been used for analyzing multiple time series [36], [37]. TRMF [27] is a temporally regularized matrix factorization approach capable of prediction (unlike previous MF approaches) while learning the temporal dependencies via an auto-regressive temporal regularizer in a data-driven fashion. A matrix factorization approach is essentially a global approach where dependencies across sequences are captured. An extension of TRMF is considered in DEEPGLO [26] which in addition to global features also considers capturing local per time-series characteristics. It uses a TCN for regularization (during MF) and prediction and can potentially capture (global) non-linear dependencies unlike TRMF. It then combines these global predictions locally using another TCN.